tend to have higher miR-155 expressions compared to mutated CLLs (p=0.09). Global expression profiling identified a set of genes differentially expressed between CLLs with high and low miR-155 levels. Among the 8 genes detected above the significance threshold after multiple comparison corrections, 2 were down-regulated and 6 were up-regulated, including *BIC*, the miR-155 precursor. One of the two down-regulated genes, ZNF652, encodes a potential tumor suppressor with transcription repressor activity and harbors two miR-155 binding sites. Both its mRNA and protein levels negatively correlate with miR-155 levels. In addition, reporter assays demonstrated specific interaction of miR-155 with its 3' untranslated region. High miR-155 in CLL is also associated with a higher level (~8 fold) of CB1 cannibinoid receptor (CNR1) mRNA and a lower (~6 to 30 fold) Kruppel-like factor (KLF3) mRNA expression.
Conclusions: ~40% of CLL over-express miR-155. Our study identified a putative miR-155 target gene that is likely to mediate the pathogenic function of miR-155 in CLL. Studies of other differentially expressed genes may uncover novel mechanisms of miR-155 over-expression in CLL.

1325 Phospho-p70s6k and cdc2/cdk1 Are Associated with Diffuse Large B-Cell Lymphoma and Are Potential Targets for Combination Chemotherapy

MY Zhao, A Auerbach, A DCosta, AP Rapoport, AM Burger, F Jiang, SA Stass, AK Sands, N Aguilera, EA Sausville, XF Zhao. University of Maryland School of Medicine, Baltimore, MD; Armed Forces Institute of Pathology, Washington, DC; University of Maryland Marlene and Stewart Greenebaum Cancer Center, Baltimore, MD; University at Buffalo, SUNY, Buffalo, NY.
Background: Diffuse large B-cell lymphoma (DLBCL) is the most common non-Hodgkin lymphoma in adults. However, only 40-60% of the DLBCL patients respond to the current standard therapy and recurrence after the initial remission is quite common. This study was to identify and evaluate novel molecular targets for the development of novel combination chemotherapy to treat the refractory and recurrent DLBCL.
Design: Lymphoma samples from 38 cases of primary and recurrent DLBCL were analyzed using real time quantitative PCR of the *RPS6KB1* and *CDC2* genes, and immunohistochemistry for their gene products p70S6K/p85S6K and cdc2/cdk1. The Farage, Karpas422, Pfeiffer and Toledo DLBCL cell lines were subsequently treated with combined rapamycin and UCN-01. The cell proliferation, apoptosis and cell cycle progression were analyzed after the drug treatment. Several key protein kinases involved in the PI3K/Akt/mTOR pathway, apoptosis and cell cycle progression were analyzed after the drug treatment.
Results: Amplification of *RPS6KB1* and *CDC2* genes was found in both primary and recurrent DLBCL. Moreover, the vast majority of these lymphomas (~94%) were strongly positive for phospho-p70S6K and cdc2/cdk1 proteins. Combination of rapamycin and UCN-01 (R+U) synergistically inhibited the DLBCL cell proliferation by inducing G1 arrest as well as apoptosis of the DLBCL cells through suppressing the phosphorylation of p70S6K/p85S6K and *CDC2* expression.
Conclusions: The *RPS6KB1* and *CDC2* overexpression is common in DLBCL. Simultaneously targeting the *RPS6KB1* and *CDC2* products phospho-p70S6K/p85S6K and cdc2/cdk1 is very effective in inhibiting DLBCL proliferation and overcoming drug resistance. This work suggests that multi-level inhibition of PI3K/Akt/mTOR pathway and double block of cell cycle progression are effective strategies for the DLBCL combination chemotherapy.

1326 Acute Erythroid Leukemias – Histologic, Cytogenetic and Molecular Characterization

Z Zuo, A Kasyan, P Chandra, J Medeiros, H Koeppen. University of Texas M.D. Anderson Cancer Center, Houston, TX.
Background: Acute erythroid leukemias (AEL) are uncommon types of acute myeloid leukemias with markedly heterogeneous morphologic, immunophenotypic and molecular features.
Design: We reviewed the clinical, histologic, cytogenetic and molecular data of 47 patients with AEL seen at our institution. All cases strictly met the criteria outlined in the WHO classification . Molecular studies included mutational analysis for Ras, KIT and FLT3 genes.
Results: The male to female ratio was 3.7, The mean age of the patients was 56 years with a range from 18 to 84. 80% were classified as primary AEL, while the remaining cases arose in patients with an antecedent MDS. Morphologically, the bone marrow was hypercellular (mean cellularity of 73%) with mean bone marrow and peripheral blood blast counts of 45% of non-erythroid precursors and 8%, respectively. Dysplastic changes in the erythroid, megakaryocytic and granulocytic lineages were seen in 84%, 55% and 31%, respectively; ringed sideroblasts were seen in 6% of cases. Two cases fulfilled the WHO criteria of pure erythroleukemia. Karyotypic abnormalities were seen in 67% of cases; 18% demonstrated a single chromosomal abnormality and 49% showed complex changes involving two or more chromosomes. Aberrancies of chromosome 5 (33%), 7 (35%) and 11 (16%) were seen in the context of complex cytogenetic abnormalities. Trisomy 8 represented 50% of cases with a single chromosomal abnormality. Mutations of the FLT3 gene were seen in 2 of 36 patients (one internal tandem duplication, one D835 mutation). None of the cases showed mutations in the RAS or KIT genes. The average survival of patients with a diploid karyotype, a single cytogenetic abnormality or complex cytogenetic changes were 18.5, 20 and 7.6 months, respectively. Statistical analysis revealed that patients with complex cytogenetics had significantly shorter survival when compared to patients a with diploid karyotype (p=0.045) or patients with a single chromosomal abnormality (p=0.017). The two patients with pure erythroid leukemia showed survival times of 4 months and less than 12 months, respectively, complex cytogenetic abnormalities including monosomy 5 and 7 and trisomy 8 and wildtype FLT3 and RAS genes.
Conclusions: Our results demonstrate a high incidence of complex karyotypic abnormalities in AEL and a low frequency of FLT3, KIT or RAS gene mutations; the karyotypic changes are similar to those seen in MDS. Further characterization of AEL will allow a distinction from or inclusion in the appropriate categories of MDS.

Infections

1327 Plasmodium Vivax Malaria: A Native American Disease

MJ Allison, S Guillen, E Gerszten. MCV Campus-VCU, Richmond, VA; Instituto Mallqui, El Algarrobal, Moquegua, Peru.
Background: Malaria is probably one of the most ancient human diseases. It is currently on the increase with half a billion cases in 2007/in 106 different countries. Whereas Pl. falciparum was a recent import carried by imported African slaves, Pl. vivax may well be an American resident for thousands of years.
Design: This current study was the examination of 155 spleens or livers from peruvian mummies belonging to seven cultural groups dating from 3000 to 600 years before present (B.P.) They were studied using U.S.Biological antibodies Pl.vivax 75/76 and Pl.falciparum 70/71 with ELISA in situ hybridization using a Biogenex Alkaline Phosphatase conjugated Streptaviden Reagent System. Histological sections were cut and stained with H&E for malaria pigment.
Results: Table 1 shows the results:

Culture	Years B.P.	No. Pl. vivax 4+	%
Azapa	3000	23	74
Alta Ramirez	2500	17	47
Cabuza	1750	49	67
Twanaku	1200	19	63
Chiribaya	1074	19	68
Huari	1000	14	71
Inca	600	14	79

Pl falciparum had 10 1+ that probably was a cross reaction with a positive 4+vivax.

Malaria type pigment was seen in about 30% of the slides of H&E.

Conclusions: Studies by Sulzier et al in 1975 on a group of isolated Campa Indian showed a high rate of malaria (63%-85%) with an etiology of only Pl.malariae and Pl. vivax . no Pl. falciparum was found. These two species are said to have evolved from a primate and cross react with some monkey malaria species. Oliveira, 1995, found 17 species of South American monkeys positive for malaria with an infection rate 2.1% - 59%. the red howler monkey was among the highest. Some monkey malaria can be contracted by humans, Howler monkey mummies are found in human cemeteries and were probably pets when the mother was hunted and killed locally in coastal valleys for food. One had his food dish with him. As coastal valley forests were cut for agriculture and coastal monkeys were all killed for food the only monkeys ar now mainly in the Amazon. Currently this practice is in effect in Columbia. Human malaria was a common disease in Pre Columbian Peru and may have had its origen in local monkey malaria.

1328 Clinical, Pathological and Immunohistological Study of Tularemic Skin Lesion and Lymphadenopathy

S Asano, M Kojima, F Shinya, H Fujita. Iwaki Kyoritsu General Hospital, Iwaki, Fukushima, Japan; Gunma Cancer Center Hospital, Ohta, Gunma, Japan; Ohara General Hospital, Fukushima, Japan.
Background: Tularemia is an infectious disease caused Francisella tularensis-infected hare. It has been well known that hare-cooking persons suffered from regional lymphadenopathy. But, there were little reports concerning skin lesions in contrast to lymph node lesions. In this section, we show relationship between tularemic skin lesion and regional lymphadenopathy.
Design: Nineteen cases of finger skin lesions, two tonsills and fifty-four cases of lymph nodes of tularemia are clinico-pathologically studied by histology and immunohistology. We analyzed relationship between time-course and skin lesions or lymphadenopathy.
Results: (1).Serum antibody titer; It shows positivity at the first week and reaches the peak around the third week. The positive reaction persists till the twentieth week after infection. (2).Skin; Inflammatory cells and small necrotic focus appear in the subcutaneous site till the second week after infection. Through the second to the sixth week, it appears ulcers and there are a lot of antigen presenting cells such as lymphocytes and dendritic cells in dilated lymph vessels in dermis. There are many small epithelioid granulomas with central necrosis in dermis as detected in subcutaneous. After the sixth week, inflammatory cells increase and it appears irregular shaped fused granulomas with central homogenous lesions in subcutaneous. (3). Lymph node; It appears primitive abscess surrounded by rough arranged mononuclear cells and histiocytic cells till the second week after infection. Many small epithelioid granulomas with central necrosis and aggregation of CD20+ lymphocytes contacted with granulomas are detected through the lymph node till the sixth week. CD4+ lymphocytes are richer than CD8+ cells through granulomas. After the sixth week, there appear granulomas with central caseous necrosis like lesions and aggregation of CD20+ lymphocytes as early phase.
Conclusions: The bacteria enter from the finger skin immediately after contact to the infected hare and it makes abscess forming granulomatous lesion in skin and regional lymph nodes. It may conclude that regional lymph node is draining from the involved cutaneous sites via lymph vessel and the antibody production period coincide

with aggregation of CD20+ lymphocytes in lymph nodes. In addition, tularemic lymphadenopathy is a subacute type of dermatopathic lymphadenopathy.

1329 Tubular Basement Membrane Deposits of C4d in Biopsies with BK Virus (BKV) Nephropathy (BKN)

I Batal, H Zainah, S Stockhausen, A Basu, H Tan, R Shapiro, P Randhawa. University of Pittsburgh Medical Center, Pittsburgh, PA.

Background: BKN has recently been associated with immune complex deposits in the tubular basement membranes (TBM). This study evaluated the deposition of complement degradation product C4d as a potential marker for this phenomenon and investigated if BKV activation can per se lead to C4d deposition in peritubular capillaries (PTC).

Design: We retrospectively examined 113 renal allograft biopsies from 52 kidney transplant recipients with a history of BKV activation defined as an episode of BK viruria (VU). All biopsies had either BKN, or had been performed within 14 days of paired urine and plasma PCR for BKV DNA. The biopsy samples were classified into 4 groups: BKV negative (NEG) (n=37), VU (n=53), viremia (VM) (n=7), and BKN (n=16). Immunohistochemistry for polyclonal C4d (ALPCO Diagnostics, Windham, NH) was performed on formalin fixed paraffin embedded biopsies. PTC and TBM C4d deposits were semi-quantitatively graded (0-3) corresponding to negative, minimal, focal, and diffuse staining, respectively. Bowman's capsule (BC) deposits were recorded as present or absent.

Results: Diffuse PTC staining was observed only in NEG and VU samples [4/37(11%) and 9/53(17%)], while focal staining was observed in all groups [13/37(35%) NEG, 9/53(17%) VU, 1/7(14%) VM, and 4/16(25%) BKN]. PTC C4d scores in VM (0.29 +/-0.76) and BKN (0.56 +/-0.89) groups were significantly lower than the VU group (1.15 +/-1.09, p=0.035 vs. VM, p=0.046 vs. BKN) and tended to be lower than the NEG group (1.19 +/-0.8, p=0.052 vs. VM and p=0.064 vs. BKN). TBM staining was a rare phenomenon that was, in its diffuse form, limited to BKN group 4/16 (25%). Focal TBM staining was observed in 2/16 (12.5%) BKN and 1/37(3%) NEG cases. TBM C4d scores were significantly higher in the BKN group (1.2 +/-1.32) compared to both NEG (0.054 +/-0.33, p=0.017), and VU (0.0 +/-0.0, p=0.008) groups. Similarly, a higher proportion of BC staining was observed in BKN samples (5/16) compared to both NEG (2/36, p=0.023) and VU (4/51, p=0.03) groups. Within BKN samples, biopsies with TBM deposits had higher percentages of infected tubular epithelial cells (12.1 +/-7.6 vs. 4.4 +/-5.0, p=0.03) and a trend toward higher Banff interstitial inflammation scores (2.7+/-0.5 vs. 2.11+/-0.6, p=0.09) compared with BKN biopsies with no TBM deposits.

Conclusions: A subset of biopsies with BKN is associated with C4d deposits in TBM but not PTC. Biopsies with TBM C4d have more pronounced viral cytopathic effect than those without demonstrable C4d.

1330 Phaeohyphomycosis Infections in Solid Organ Transplant Recipients – The Largest Single Institution Experience

EN Beckman, JB Garcia-Diaz, GE Loss, JS Schieffelim, CG Staffeld-Coit, JC Garces, RA Keller, GA Pankey. Ochsner Clinic Foundation, New Orleans, LA.

Background: Phaeohypomycotic infections are relatively common in solid organ transplant recipients. Awareness of the characteristic morphology is important in prompt treatment and if the lesion was not cultured.

Design: Specimens were reviewed years 1988-2005 from 24 patients with solid organ transplants and Phaeohypomycosis infection.

Results: Biopsy material from the skin and subcutaneous tissue was most common (38 separate specimen.) The typical histologic appearance was one of purulent granulomas with central acute inflammation, surrounding granulomatous change with varying number of giant cells and peripheral inflammaton and fibrosis. In older lesions, the granulomatous quality was less-well defined, and there was more fibrosis and chronic inflammation. Varying numbers of brown fungal forms were evident with H&E stains. 25 of the 38 had visible brown fungus, although in a minority of cases the organisms were only faintly brown. The most intensely brown structures were yeast. In 13 specimens, the organisms were only seen with a special stain. Fungi were consistently positive with the GMS, PAS, and Fontana-Masson stains, although the GMS stain was the one commonly used. Fungal forms varied and include forms that were simple mycelial, mycelial with bulbous distention, mycelial and yeast, and only yeast. Fungal forms, especially mycelial, tended to be within giant cells. 8 of the 38 skin and subcutaneous specimens consisted of only deeper tissue. Of the 30 specimens that were not exclusively deep, pseudoepitheliomatous hyperplasia of the epidermis was present in 20. That hyperplasia was mild in 8, moderate in 4, and pronounced in 8. In one specimen this proliferation was very difficult to distinguish from well-differentiated squamous carcinoma. A brain and a lung specimen both had purulent granulomas with brown fungi. 2 specimens were lung cytology specimens which contained brown fungi. Fungi of al specimen were compatible with forms of Phaeohypomycosis (culture confirmed in 20 patients).

Conclusions: In cases of possible Phaeohypyhomycosis infection, culture of the specimen is highly desirable. Still, definitive diagnosis can usually be made based upon the morphology.

1331 Adiponectin Levels during the Septic Response to *B. anthracis* Sterne Strain in Baboons

HG Cohen, S Kurosawa, DJ Stearns-Kurosawa. Boston University School of Medicine, Boston, MA; College of Veterinary Sciences, Oklahoma State University, Stillwater, OK.

Background: Adiponectin is a soluble mediator from white adipose tissue known to improve insulin sensitivity and have cardioprotective functions. During sepsis, dysfunctional insulin metabolism contributes to disease severity. During a septic response, however, the role of adiponectin is not clear and data are conflicting as to a protective or inflammatory role. Baboons are a validated animal model of sepsis and challenge with Gram positive *Bacillus anthracis* Sterne strain results in the pathophysiologic responses typical of sepsis. The question of whether changes in adiponectin levels corresponded to survival or an inflammatory response in this model were evaluated.

Design: Anesthetized baboons (*Papio cynocephalus anubis;* 6-8kg; n=13*)* were challenged by infusion with toxigenic Gram negative *Bacillus anthracis* Sterne strain (0.005-9.5 x 10^9 CFU/kg) using published methods (*Am J Path* 169:433, 2006). Blood was sampled at various time points and plasma was stored at -80ºC until assayed. Adiponectin values were determined by ELISA (R&D Systems) that recognizes the globular domain of human adiponectin. Plasma TNFα levels were determined by ELISA using published methods.

Results: Baseline adiponectin levels varied between animals with Mean ±SD = 40.7±17.7 ug/ml (Range 8.1- 77.9). Adiponectin levels did not correlate with TNFα levels after challenge with *B.anthracis* Sterne strain. Increasing bacteria challenge led to increased TNFα at T(2hrs) post-challenge, but adiponectin levels did not change significantly at <24hrs. With low challenge (<7x10^8CFU/kg) and modest inflammatory response, adiponectin levels increased 35-115% between day 1-7 post-challenge. Adiponectin levels at before challenge were not related to survival (p=0.19), but 7 day survivors had higher adiponectin levels than those who succumbed at 2-5 days (52.1 ±16.4 *vs* 33.4 ± 14.7 ug/ml, p<0.05; n=12) despite similar bacterial challenge doses.

Conclusions: An early TNFa inflammatory response due to septic challenge did not result in corresponding changes in adiponectin levels, suggesting that release of adiponectin from adipose tissue may be regulated locally, but is not mediated by systemic TNFα levels during sepsis. Adiponectin levels may play a role in a protective function late in the septic response because survivors tended to have higher adiponectin levels at day seven post-challenge. [NIH UO1AI075386 (SK)]

1332 Recovery of Lymphoid Tissue Architecture and CD4 Cell Count Could Be Limited by Fibrotic Changes in HIV+ Patients under Antiretroviral Treatment

A Diaz, A Mozos, F Garcia, M Caballero, A Martinez, JM Gatell, L Alos. Hospital Clinic, IDIBAPS, UB, Barcelona, Spain.

Background: Although peripheral blood viral load and T-cell subsets are usually used for monitoring HIV infection, key pathogenesis events take place in lymphoid tissues. Lymphoid tissue (LT) indemnity is crucial for the immunological recovery in HIV-infected patients under highly active antiretroviral therapy (HAART). The aim of our study was to evaluate the changes of LT architecture and CD4+ cell counts in HIV patients receiving HAART.

Design: Tonsillar biopsies were performed in 7 patients with chronic asymptomatic HIV-1 infection before initiating HAART and 25 after receiving HAART for a long time (from 17 to 112 months). Five tonsillar resections of HIV-negative individuals were used as controls. From formalin-fixed and paraffin-embedded tissue we performed in each case H&E, Masson trichrome and immunostain for CD4 (Novocastra, 1F6). Quantitative image analysis was used to assess LT architecture, with the measurement of the proportion of LT occupied by follicular areas (FA), collagen deposition (fibrosis), and the mean interfollicular CD4+ cell count per μm^2.

Results: Before HAART, LT showed effacement of the architecture, with absence or small follicle structures (mean proportion of FA of 0.045). After initiating HAART, there was a recovery of LT architecture (mean FA of 0.157), which correlated with a significant increase of interfollicular CD4+ cells (p<0.001). However the CD4+ cell count did not reach the CD4+cell count of HIV- patients. We observed a higher proportion of fibrosis in tonsillar biopsies of patients receiving HAART (median 5%), compared to those from HIV- patients. We also found that the biopsies with a higher amount of fibrosis had a lower CD4+ cells, although this finding was not significant. There was a significant increase of LT fibrosis in patients receiving reverse transcriptase inhibitors when compared to those receiving protease inhibitors (p=0.029).

Conclusions: The treatment with HAART produces a significant recovery of LT architecture and CD4+ cells but it does not reach the CD4+ cell count of HIV- patients LT, even after a long time of treatment. We have found for the first time a higher amount of collagen deposition in LT of patients receiving reverse transcriptase inhibitors, compared to those receiving protease inhibitors. This fact could limit the immune recovery in these patients.

1333 Detection of *Clostridium difficile* Toxins in Stools and Presence of the Bacteria in Tissues in a Pediatric Population

J Guarner, J Bhatnagar, T Jones, E Schemankewitz, SR Zaki. Emory University, Atlanta, GA; Centers for Disease Control and Prevention, Atlanta, GA; Children's Healthcare of Atlanta, Atlanta, GA.

Background: Pseudomembranous colitis has been associated with *Clostridium difficile* overgrowth after use of broad-spectrum antibiotics. Even though *C. difficile* toxin is frequently found in the stool of children, pseudomembranous colitis is rare, suggesting that bacteria are colonizing the gut without producing pathology. The objective of this study was to correlate the presence of *C. difficile* toxin in stool and presence of gastrointestinal pathology with detection of *C. difficile* in pediatric tissue samples.

Design: We performed a retrospective chart review of 12 patients who had intestinal tissue obtained around the time stools were positive for *C. difficile* toxins using a kit that employs a monoclonal anti-toxin A antibody and a polyclonal anti-toxin B antibody. Paraffin embedded tissues were studied by an immunohistochemical assay (IHC) using a polyclonal anti-*C. difficile* antibody and by a PCR assay specific for *C. difficile* toxin B gene.

Results: The median age was 8 years (range 4 weeks to 17 years) and 5 were female. The median amount of time between the positive *C. difficile* toxin in stool and obtaining the tissue was 3 days (range same day to 8 weeks). The reason antibiotics were prescribed included diarrhea (4 children), fever (3), abdominal pain (2), vomiting (1), cellulitis (1), and sepsis (1). Nine patients underwent endoscopy which showed normal mucosa

(2), erythema and friability (2), erosions (2), increased mucous production (1), and pseudomembranes (1). Two children underwent laparotomies for either obstruction or resection of necrotic bowel. One child died and the intestine showed abundant pseudomembranes. Mild inflammation was observed in 7 samples, necrosis in 2, granulomatous inflammation in 1, moderate colitis in 1 and pseudomembranous colitis in 1. IHC demonstrated non-specific staining of bacilli and cocci in the lumen. PCR for the toxin B gene was negative in all cases.
Conclusions: Detection of *C. difficile* toxin in stool and non-specific staining of bacteria using IHC may relate to the use of polyclonal antibodies. No correlation was observed between immuno assays and PCR in these children. Development of tests that are specific for *C. difficile* is necessary to understand the pathogenic mechanism of the bacteria and its toxins.

1334 Chemokines Are Selectively Regulated during the Progression of Acute Inflammation

DL Horton, DG Remick. Boston University Medical School, Boston, MA.
Background: Upon traumatic or infectious injury, secreted cytokines and chemokines display distinct kinetic profiles during the inflammatory response. However, it remains unclear whether this distinction confers differential regulation of inflammation. Using human whole blood as a model system, we examined the effects of delayed DEX on LPS-induced cytokines and chemokines. We hypothesized that chemokines are selectively regulated during the progression of acute inflammation in the whole blood model.
Design: Venous blood was collected from healthy volunteers into heparinzed (10U/ml) syringes. 50 ng/ml LPS or RPMI 1640 was added to the blood in 1.5 ml Eppendorf tubes, followed by continuous mixing with 5% CO2 and ambient air at 37oC. Blood was spun at 1000 x g for 5 minutes at various time points and plasma collected and stored at –20oC for later cytokine analysis. For dex experiments, 10-6M dex was added to blood simultaneously with LPS at time 0, or after 6 h.r LPS stimulation. Plasma was collected at various time points and stored until later analysis. These studies have been approved by the Institutional Review Board of Boston University.
Results: Blood gas analysis revealed unchanged partial pressure of O2 for up to 24 hours, while pCO2 increased from 50 ± 3 to 74 ± 4 mmHg. Glucose and pH decreased significantly (99 ± 6 to 0.5±0.2 mg/dL, and 7.3±0.02 to 7.0±0.02, respectively) between 0 and 24 h. Cellular viability remained unchanged after 24 hours of incubation with DEX. LPS (50 ng/ml) stimulation induced TNF, IL-1, and IL-6, which peaked by 6 hours. In contrast, chemokines (GRO and IL-8) increased steadily up to 24 hours. Maximal TNF, IL-1, and IL-6 mRNA levels were observed at 2 hours and were undetectable by 6 hours. GRO and IL-8 mRNA displayed an initial peak at 2 h, and subsequently decreased by 12 hours. Between 12 and 24 hours, chemokine mRNA increased steadily. Simultaneous DEX (10-6M) and LPS resulted in significant suppression of cytokines and chemokines at 24 hours. However, delaying DEX until 6 hours after LPS abrogated its suppression of TNF, IL-1, and IL-6. In contrast, delayed DEX significantly suppressed both GRO and IL-8 levels.
Conclusions: In conclusion, these data suggest that the regulation of progressive inflammation occurs via modulation of chemokines, but not cytokines, in the whole blood model of acute inflammation. Thus, future experiments should be aimed at targeting therapies specifically to chemokines.

1335 Clinical and Morphological Analysis of Lymphoid Interstitial Pneumonia (LIP) Variants in Adult HIV Patients: A Retrospective Study of 25 Cases

R Hughes, J Park, N Edgerton, N Vogenthaler, MB Mosunjac, MI Mosunjac. Emory University, Grady Memorial Hospital, Atlanta, GA.
Background: The diagnosis of LIP encompasses both clinical and pathological patterns of pulmonary disease characterized by a diffuse interstitial lymphoid infiltrate. Its association with HIV has been previously demonstrated, and recently the incidence of HIV-associated LIP has been on the rise. This trend has been primarily observed in children with AIDS. However in the adult HIV population, the incidence of LIP remains stable. Here, we describe the clinical, laboratory and morphological features of the largest series of HIV-associated LIP in adult patients.
Design: Twenty-five lung biopsies with a diagnosis of LIP were identified between 1992 and 2008. Pathology reports, H&E slides and available fungal and immunohistochemical stains (GMS, CD3, CD20) were reviewed. Clinical and laboratory data data was obtained from the patients' charts.
Results: Of 25 patients, there were 4 females and 21 males with an average age of 38.4 years. Sixty-four percent of the patients lacked documented risk factors for HIV, while thirty-four percent of patients had a history of drug abuse. The average duration of HIV infection at the time of LIP diagnosis was 79 months. Morphologically, two LIP patterns were identified; 13 cases contained nodular lymphoid infiltrates, and 12 exhibited a diffuse interstitial pattern. Of the four female patients, three showed the diffuse interstitial pattern. Frequently, the nodular pattern was clinically mistaken as miliary TB or metastatic tumor (61.5%). CD8 lymphocytosis was observed in more than 75% of cases with an average CD8 count of 1541 cells/mm^3. The average CD4 count was 282 cells/mm^3 with an average viral load of 242,270 copies/mL. There was no statistical significance between morphological patterns of LIP and CD4/CD8 count, duration of HIV, or risk factors.
Conclusions: Here we present the largest series of LIP in adult HIV patients. All of the patients showed a long duration of HIV infection with significant CD8 lymphocytosis. The most prominent risk factor identified was drug abuse. Of the four female patients, three showed the diffuse interstitial pattern. There was no significant distinction in laboratory or clinical findings between the two morphological LIP patterns. The nodular pattern was clinically more often diagnosed as miliary TB or metastatic tumor nodules.

1336 Soft Tissue Rosai Dorfman Disease: A Large Series with Detection of SV40 Antigen in Select Cases

MK Klassen-Fischer, A Auerbach, W Al-Daraji, JC Fanburg-Smith. Armed Forces Institute of Pathology, Washington, DC.
Background: Soft tissue Rosai-Dorfman Disease (STRDD) is rare, previously reported only as single cases and few series. Simian virus 40 (SV40), a polyomavirus, has been identified in lymphoid processes and has a controversial role in neoplasia etiology. Occasional cytoplasmic pink granular inclusions led us to explore a viral etiology.
Design: Only unpublished STRDD from our files with adequate material, soft tissue location, and diagnostic confirmation, were included; IHC and follow-up obtained.
Results: 19 STRDD patients, 5 male and 14 female, had 34 lesions; six with 2-6 lesions. Ages ranged from 8-81 years, mean and median 43 years. STRDD locations: trunk or proximal extremity (n=20), distal extremity (n=9), "abdominal" (n=3), face (n=1), and unknown subcutis site (n=1). Sizes ranged 0.5 to 13.7 cm (median 2.4 cm). Previous disease included lymphoma, buttocks injection site, diabetes and hypothyroidism, and radiation for chronic dermopathy. No patients had a preceding or concurrent known viral infection; only one had lymphadenopathy. None were known to be immunocompromised. All STRDD were rapidly growing. Initial pathologic diagnosis ranged from RDD or inflammatory pseudotumor to inflammatory malignant fibrous histiocytoma. Grossly STRDD were multilobulated, tan-yellow and firm; morphologically, circumscribed and subcutaneous. All had sheets of polygonal histiocytes with abundant pale eosinophilic cytoplasm, emperipolesis, plasma cells and lymphocytes scattered and within clusters. Focal spindle cell change and mild pleomorphism were each observed in 3 patients; 2 had focal necrosis, none mitoses. Small granular pink cytoplasmic inclusions were observed. By IHC, all STRDD were positive for S100 protein, negative for CD1a, EBV and LMP, yet 3 (all abdominal, one multicentric) of 9 were focally positive for cytoplasmic SV40. All were treated by local excision. Follow-up on 15 patients over 8-16 years revealed recurrence in four patients with persistent multiple lesions, one with abdominal location. There were no metastases.
Conclusions: STRDD is a rapidly evolving, mostly solitary and non-recurrent trunk and proximal extremity subcutaneous lesion in middle aged females. One-third can have persistent multicentric disease. It is important to recognize STRDD, to separate it from malignancy. EBV/LMP were negative but SV40 was positive in 3 patients with abdominal STRDD, one with multicentric persistent disease. The relationship of SV40 to the evolution of abdominal STRDD should be further explored.

1337 AIDS-Associated Hemophagocytic Syndrome: A Study of 100 Autopsy Cases

M Naghashpour, EM Sagatys, R Smith, HD Cualing. Moffitt Cancer Center and Research Institute, Tampa, FL; University of Cincinnati, Cincinnati, OH.
Background: Hemophagocytic syndrome (HPS) is a clinicopathologic entity characterized by proliferation of macrophages with hemophagocytosis throughout the reticuloendothelial system. Its pathogenesis is thought to be related to defects of NK- and cytotoxic T-cells, and an altered cytokine milieu. HPS may be primary or secondary (acquired). Acquired HPS has been described in association with various infections, malignancy, collagen vascular disease and immunodefficient states. Clinical presentation is that of a systemic illness, typically characterized by fever, cytopenias and splenomegaly.
Design: A total of 100 consecutive adult AIDS autopsy records were identified. Cases with splenomegaly (>500 grams) were selected. Massive splenomegaly was defined as splenic weight >1000 grams; we prefer the term "macrosplenomegaly". Tissue sections were stained by conventional histologic stains (H&E, PAS, Giemsa and silver stains) to investigate the etiology of splenomegaly. Immunohistochemical stains and in situ hybridization for viral RNA, and electronmicroscopy for the examination of utrastructure were also performed.
Results: Our analysis revealed fourteen cases with splenomegaly (14%), of which six cases showed massive splenomegaly (6%). Five of these six cases had histologic evidence of histiocytosis with hemophagocytosis in multiple organs including spleen. Mortality preceded by intractable fever, cytopenias unresponsive to blood product transfusions, and multi-organ systemic dysfunction. The clinical signs and symptoms in comibation with the morphological findings were characteristic and diagnostic of HPS. In four cases (4%), an underlying opportunistic infection (EBV and CMV) and/or a virus-associated malignancy (Kaposi sarcoma) were present. In one patient (1%), no underlying malignancy or opportunistic co-infection was found.
Conclusions: We found HPS and associated massive splenomegaly in 5 of 100 AIDS autopsy cases. In the setting of HIV infection, impaired cytotoxic T lymphocyte function, selected NK-cell depletion, and/or opportunistic infections in conjunction with an altered cytokine milieu may explain the predisposition to developing HPS. In our study, HIV infection in conjunction with opportunistic infectious agents (EBV and CMV) and/or malignancy (Kaposi sarcoma) is implicated to have precipitated 4 of 5 HPS cases. HIV infection alone (1 of 5 cases) may also trigger life-threatening HPS with associated macrosplenomegaly and severe cytopenias.

1338 Pediatric Bacterial Lymphadenitis: An Eight-Year Experience at a Large Academic Center

FG Nunes, D Itani, SL Cook, R Verrall, C Stratton, CA Mosse. Vanderbilt University Medical Center, Nashville, TN.
Background: Infectious lymphadenitis is a common disease in children with numerous etiologies. An accurate differential from a lymph node biopsy can expedite diagnosis and minimize ancillary testing. There are few published case series that compare the histopathology of uncommon pathogens such as *Francisella tularensis* with more common agents.
Design: We reviewed all lymph node biopsies showing lymphadenitis in immunocompetent children under the age of 15, from July 2000 to June 2008. Age,

site, pattern of inflammation, and results of AFB stains, culture and DNA hybridization were assessed.

Results: Thirty-five cases fulfilled the inclusion criteria. These represented 21 cases of *Mycobacterium avium* complex (MAC) (60%), 1 *Mycobacterium fortuitum* (3%), 7 *Bartonella henselae* (20%), 2 *Yersinia entercolitica* (7%), 1 *Francisella tularensis* (3%) and 1 *Streptococcus pyogenes* (3%). The mean age of mycobacterial patients was 2.2 years old; 9 (42%) were found in submental lymph nodes and 4 out of 21 (19%) showed AFB positivity. Eighteen cases (86%) had caseating granulomas as their sole histopathologic finding. Conversely, *Bartonella* and *Francisella* affected older children (9.8 yo mean) and typically showed extensive granulomatous and suppurative necrosis. *Streptococcus* and *Yersinia* had extensive suppurative necrosis as the only finding (see table). Interestingly, *Yersinia* was found in an inguinal lymph node and not in a mesenteric lymph node as usually described.

	Test	# Cases	Type of necrosis					
			Suppurative			Granulomatous		
			Extensive	Microabscesses	Stellate microabscesses	Poorly formed	Well formed	
							Non caseating	Caseating
Mycobacterium avium	DNA probe	21		1			1	18
				1				
Mycobacterium fortuitum	DNA probe	1						1
Bartonella henselae	PCR	7		2				
				1				
							2	
			2					
Francisella tularensis	Culture	1		1				
Yersinia enterocolitica	Culture	2	1	1				
Streptococcus pyogenes	Culture	1	1					
Total		35						

= case with one feature present
= one case with two features present

Conclusions: We believe MAC should always be considered in young children with caseating granulomatous lymphadenitis. Because the sensitivity of AFB for mycobacterial infections is very low (19% in this study), molecular techniques should be regularly employed. Cat-scratch disease and tularemia should be investigated in older children presenting with both abscesses and granulomas, notwithstanding the lack of stellate microabscesses. Yersiniosis should be suspected in young children presenting with extensive suppurative necrotizing lymphadenitis. These distinct clinical and histological patterns may help direct ancillary testing to minimize expense and time to diagnosis.

1339 STX-1 Non-Human Primate Toxemia Model: Circulating Leukocyte mRNA Changes Coincide with Disease Onset

JF Papin, DJ Stearns-Kurosawa, V Collins, S Freeman, G Peer, S Kurosawa. Boston University School of Medicine, Boston, MA; University of Oklahoma Health Sciences Center, Oklahoma City, OK; College of Veterinary Sciences, Oklahoma State University, Stillwater, OK.

Background: Enterohemorrhagic *Escherichia coli* (*EHEC*) that produce Shiga-like toxins are an important public health problem and a biodefense concern. EHEC from contaminated water and food lead to the severe conditions of hemorrhagic colitis and hemolytic-uremic syndrome (HUS). The young and elderly are especially vulnerable and HUS survivors often suffer permanent renal damage. Antibiotics are contraindicated, and there is no specific treatment, other than general supportive care. The primary virulence factors are circulating Shiga-like toxins 1 and 2 (STX-1, STX-2). To accelerate the development of novel therapeutics, we are developing and characterizing a pre-clinical, non-human primate model for Shiga toxemia.

Design: Toxemia was induced by i.v. 100ng/kg STX-1 to anesthetized baboons, *Papio cynocephalus* (n=5) with lethal outcome at 48 ~72 hours. Quantitative PCR (qPCR) assays were designed from baboon sequences to follow expression of TNFα, IL-6, IL-8, IL-12p35, MIP-1α, MCP-1, Elastase-2 (neutrophil elastase), and VEGF in the blood during STX-1 toxemia. RNA was isolated from peripheral blood leukocytes (PBL) obtained from timed heparinized blood samples and used to generate target cDNA for the qPCR.

Results: The clinical manifestations included bloody diarrhea, oliguria, thrombocytopenia without fibrinogen depletion, microangiopathic hemolytic anemia (MAHA) with schistocytes. There was increased expression of TNFα (4/5 baboons), IL-6 (3/5), IL-8 (5/5), MIP-1α(5/5), and MCP-1 (4/5) in the PBLs. The expression of TNFα, IL-6, IL-8, MIP-1α, Elastase-2, and MCP-1 all showed marked increase at 24 hours post exposure that continued to increase through the 48-hour time point. On average, we observed ~5 to 10 fold increases in expression in these cytokines, with the exception of MCP-1 which demonstrated a ~20-40 fold increase.

Conclusions: The clinical manifestations in our baboon model recapitulate many of the characteristics in patients. Our findings in the baboon model show a marked increase of pro-inflammatory cytokine expressions in PBLs at ~24 to 48 hours-post exposure to STX1. Notably, this burst of cytokine expression corresponds to the onset of thrombocytopenia, oliguria and MAHA, suggesting a direct role in the pathogenesis. [NIH UO1AI075386 (SK)]

1340 A Multidisciplinary Approach to Anal Cytology in HIV+ Males: A VAMC Experience

NM Patil, HX Bui, JP Reynolds, S Samaan, D Moore, V Skeen, AG Smulian, J Robertson. VAMC, Cincinnati; U of Cincinnati, Cincinnati.

Background: HIV patients are at greater risk of Anal Intraepithelial Neoplasia (AIN) and anal cancer. Our VA-based screening program involves cytologic liquid based preps (LBP), high resolution anoscopy (HRA), and histologic examination of HRA-guided biopsies. High risk HPV DNA testing (hrHPV) and IHC for p16, p53, p63, Ki67 have been used as biomarkers for detection of HSIL. The aim of our study is to analyze the performance of molecular testing in diagnosing HSIL.

Design: 262 screening anal LBPs were collected from HIV+ men during 2005-2007 and assessed with the Bethesda criteria. 34 HRA-guided biopsies were selected for IHC stains; biopsies were reviewed independently by two pathologists. Of these, 27 biopsies had sufficient tissue for additional slides and were stained using IHC for p16 (BD Pharmagen 1:500), p53, p63 and Ki67 (Dako 1:100, 1:50, 1:200). 70 LBPs with ASCUS or higher were assessed with PCR-based hrHPV DNA testing (ARUP laboratories). The sensitivity, specificity, PPV and NPV for detecting HSIL on histology was calculated for IHC stains and hrHPV testing, and ROC curves were generated for each IHC stain.

Results: 262 LBPs analyzed; 87 were abnormal. Abnormal cytology consisted of: 24 (28%) ASCUS, 42 (48%) LSIL, 21 (24%) HSIL. Anal biopsy histology: 2 (7%) normal, 11 (41%) LSIL, 12 (44%) HSIL, 2 (7%) SCCIS. Cytology agreed with the histological diagnosis in 18/27 (66%) of samples. 70 LBPs tested for HPV: 49 had hrHPV (70%), 4 negative (6%), 17 equivocal with scant cellularity (24%).

Molecular tests for HSIL

Stain	%cutoff	%Sensitivity	%Specificity	%PPV	%NPV	ROCAUC*
HPV DNA	NA	64	33	53	44	NA
P16	≥15	71	85	50	73	0.79
P53	≥10	43	62	43	62	0.5
P63	≥60	36	38	38	36	0.45
Ki67	≥10	64	61	64	62	0.69

*ROC-AUC = ROC area under curve

Conclusions: 1) Positive hrHPV DNA testing was moderately sensitive but poorly specific for diagnosing HSIL. The high frequency of scant cellularity on LBPs reduces the utility of HPV DNA testing, decreasing it's value for detecting HSIL. 2) Based on the ROC area under the curves, p16 and Ki67 had the best diagnostic value for identifying HSIL while p53 and p63 were not useful. Detection of viral cytopathic effect in cytology and histology remain the most important means for detecting HSIL. p16 and Ki67 may have a role in supporting the diagnosis of HSIL when there is diagnostic uncertainty. 3) A multidisciplinary approach to diagnosis would be complementary to facilitate appropriate management.

1341 Histopathologic Characteristics of Granulomas Associated with Lung Malignancies: A Retrospective Study

JB Placido, VB Reddy, AJ Patel, AW Kim, M Liptay, P Gattuso. Rush University Medical Center, Chicago, IL.

Background: Sporadic reports in the literature identify the coexistence of noncaseating granulomas (sarcoid-like pattern) with hematologic malignancies as well as with solid tumors, including lung. We undertook a retrospective study of 128 cases of lung granulomas to assess the incidence as well as the histologic type of granulomas that coexist with malignancies.

Design: Review of our surgical pathology records from 1996 to 2008 identified 128 lung specimens with granulomas. The following characteristics were reviewed: Age, sex, histologic type of granulomas, and coexistance of granulomas with tumors.

Results: A total of 128 patients with lung granulomas were recorded. Seventy were female and 58 were male. The age ranged from 24 to 89, with a mean age of 59 years. Seventy-three granulomas were necrotizing, and 55 were not necrotizing. Forty-seven (36.7 %) out of 128 cases showed microorganisms (31 histoplasma, 8 aspergillus, 4 coccidioides, and 4 blastomyces). Thirty-seven (28.9 %) cases were associated with lung malignancies (19 adenocarcinomas, 7 squamous cell carcinomas, 3 carcinoids, 2 large cell carcinomas, 1 small cell carcinoma and 5 metastatic tumors). In this group of patients, 17 had caseating granulomas and 20 had noncaseating granulomas (12 calcified, 3 hyalinized, and 5 with sarcoid-like pattern). Nine (24.3%) of these cases showed microorganisms (8 histoplasma, 1 blastomyces).

Conclusions: 1. Thirty-seven (28.9 %) cases of lung granulomas were associated with malignancies. 2. The most common malignancy associated with granulomas is adenocarcinoma-- 19 (51.3 %) cases. 3. Nine (24.3 %) out of 37 cases of granulomas associated with malignancy showed microorganisms (8 histoplasma, 1 blastomyces). 4. Of the different histologic subtypes of granulomas associated with tumors, the least common was a sarcoid-like reaction (5 cases). 5. The presence of sarcoid-like reaction may represent a local immune response to tumor cells and could play an important role in the host defenses against metastatic spread. 6. The association of granulomas with malignant lung tumors poses a challenge for clinicians in differentiating granulomas versus tumor spread. Tissue biopsy is still needed in the majority of the cases to confirm the diagnosis. 7. An unusual finding is that none of the granulomas in our series was associated with mycobacterial infection.

1342 Infectious Etiology of Granulomatous Inflammation on Bone Marrow Biopsy

SS Rahman, JM Ben-Ezra. Virginia Commonwealth University Health System, Richmond, VA.

Background: Bone marrow aspiration and biopsy are commonly performed in evaluation of immunocompromised patients, especially those with AIDS/HIV. Granulomatous inflammation is identified in a subset of these biopsy cases, which consequently warrants further workup for an infectious source with histochemical stains or microbiological cultures. The infectious etiology of the granulomatous inflammation seen on bone marrow biopsy is not fully understood.

Design: We conducted a retrospective review of all adult bone marrow biopsies obtained from January 2000 through June 2008 in which both microbiological cultures of the bone marrow aspirate were collected and histochemical stains for microorganisms (GMS, PAS-Light Green, Ziehl-Neelsen) were performed. The following characteristics for each case were recorded: age, gender, HIV status and viral load, biopsy length and width, presence or absence of granulomatous inflammation, and results of histochemical stains and microbiological cultures.

Results: A total of 113 cases meeting the above criteria were reviewed. Granulomatous inflammation was identified in 47 cases (41.6%), of which 17 cases (36.2%) showed

evidence of infection by either histochemical stain or microbiologic culture. Conversely, infection was detected by stain or culture in 9 out of 66 cases (13.6%) without granulomatous inflammation (p=0.005). Of the 113 cases studied, 10 cases (8.9%) were positive for microorganisms by both histochemical stains and culture; 12 cases (10.6%) were culture-positive, stain-negative; 4 cases (3.5%) were stain-positive, culture-negative; and 87 cases (77.0%) were culture-negative, stain-negative (p<0.001). The organisms identified by culture were *Mycobacterium avium* complex (19 cases), *Histoplasma capsulatum* (2 cases), and *Cryptococcus neoformans* (1 case). There was no significant relationship between biopsy area (length x width) and granulomatous inflammation (p=0.318). In addition, there was no correlation between HIV status (+/-) and either granulomatous inflammation (p=0.114) or detection of microorganisms (p=0.147). There also was no correlation between HIV viral load and presence of granulomas (p=0.404) or infection (p=0.584).
Conclusions: The presence of granulomatous inflammation on bone marrow biopsy is associated with fungal or mycobacterial infection in a minority of cases (36.2% in our series). A combination of both histochemical stains and microbiological culture of the aspirate material is recommended for enhanced detection of occult microorganisms in immunocompromised patients.

1343 Abdominal Angiostrongyliasis: 24 Cases Diagnosed on Specimens from Surgical Emergencies

M Saravia, V Argueta, R Orozco, L Castillo. Hospital General San Juan de Dios, Guatemala, Guatemala.
Background: *Angiostrongylus costaricensis* is a nematode found in the American continent. Humans are accidental hosts. After the infection, the parasite migrate trough the intestinal wall and reach the mesenteric arteries of the ileocecal region. Most symptoms associated with *A. costaricensis* are due to an inflammatory/ischemic reaction of the tissues supplied by the affected vessels. Typically, the patient presents with acute abdominal pain. Depending upon the severity of the ischemia within the bowel, the patient can develop necrosis and even perforation. The diagnosis of angiostrongyliasis is made trough the histopathological confirmation of the parasite.
Design: We reviewed 24 histologically confirmed cases of abdominal angiostrongyliasis, from 1999 to 2008. Clinical, macroscopic and microscopic findings that could be useful for the clinician and pathologist to diagnose this disease were searched for.
Results: There were 17 male and 7 female patients; aged 1 to 74 years (mean 23.6). All cases presented to the emergency room as acute abdomen; most frenquently clinical interpreted as acute appendicitis. In 5 cases, a right lower quadrant mass was palpable. The pathological specimens derived from 6 appendectomies, 7 terminal ileum resections, 10 ileo-colic resections and 1 yeyunal resection. One patient needed re-intervention 10 weeks later due to another intestinal perforation. Macroscopically, the external surface of the specimens showed vascular congestion, fibrosis and hemorrhage. Thickening of the intestinal wall, sometimes simulating a mass, was a striking feature. Mucosal findings included 5 cases with flattening of the mucosa, 6 with ulcerations and 4 with a cobblestone pattern. Transmural necrosis or perforation was found in 14 of the 24 cases, including 1 yeyunal perforation. Histologically, abundant presence of eosinophils and vascular necrosis were always distinctive findings. The amount of eggs, larvae and adult worms varied from case to case. Some had abundant adult parasites, larvae and eggs while others needed ample sampling to find occasional eggs.
Conclusions: This is a large series of confirmed abdominal angiostrongyliasis cases reported from Guatemala. It illustrates the presentation of this disease for the clinician as well as for the surgical pathologist. Abdominal angiostrongyliasis frequently presents as an intestinal resection specimens with clinical history of acute abdomen. It is important for American pathologists to recognize it due to the increase immigration to the USA from endemic areas.

1344 Transbronchial Fine-Needle Aspiration Diagnosis of Non-Neoplastic Diseases Including Infections with Unusual Presentations

VJ Schnadig, KA Millington, VJ Cardenas. University of Texas Medical Branch, Galveston, TX.
Background: Bronchoscopy-guided transbronchial fine-needle aspiration (TBNA) is commonly used for staging and diagnosis of bronchogenic carcinoma. Little emphasis has been given to its use for diagnosis of non-neoplastic conditions. Evaluation of the utility of TBNA for diagnosis of non-neoplastic conditions, particularly for infectious and inflammatory diseases, is warranted.
Design: A computerized search of TBNA performed from January 2001 through August 2008 was done. TBNA targets included enlarged mediastinal lymph nodes and peribronchial lung lesions. Cases with diagnoses of non-neoplastic conditions were reviewed and correlated with clinical, radiologic, and culture results.
Results: Five hundred ninety-one TBNA were found. Out of these, 102 were interpreted as diagnostic of benign conditions. Seventy-five were reactive mediastinal lymph nodes. Twenty-seven benign disease processes were diagnosed. Diagnoses included granulomata (19), spindle cell granulomata (2), necrotizing inflammation (4), granulation tissue with bacteria (1) and bronchogenic cyst (1). Microorganisms were identified by cytology in 8 cases. Especially unusual and interesting diagnoses included endobronchial actinomycosis, *Mycobacteria kansasii* spindle cell granulomata and *Coccidioides immitis* mediastinal lymphadenitis. In all cases, correlation with clinical and radiologic findings and subsequent cultures were done. Diagnoses of non-neoplastic diseases excluded malignancy and directed clinicians toward use of appropriate therapy.
Conclusions: A small, but significant, number of TBNA yielded diagnoses of non-neoplastic diseases. Unusual presentations of infectious diseases were diagnosed by TBNA in a few cases and provided clinicians with information useful for patient management.

1345 Increased CXCL10 Is Associated with Reversal Reaction in Leprosy

DM Scollard, A Martinez, M Chaduvula, N Fowlkes, I Nath, B Stryjewska, DL Williams. National Hansen's Disease Programs, Baton Rouge, LA; Fundacao Oswaldo Cruz, Rio de Janeiro, Brazil; LEPRA- Blue Peter Research Centre, Hyderabad, India; Louisiana State University, Baton Rouge.
Background: The normally indolent course of leprosy is complicated in many patients by an acute, systemic inflammatory syndrome termed 'Reversal Reaction' (RR) that is a major cause of neuritis and other morbidity in leprosy. RR appears to be a spontaneous enhancement of cellular immunity, but the mechanisms underlying this clinical syndrome are unknown and no laboratory tests are available to diagnose or monitor it.
Design: Sereum was collected monthly x 12 from 20 patients in India who had borderline leprosy (10BT and 10 BL) and who had RR at some time during their course, and from 20 similar patients who did not have RR. Serum CXCL10 levels were assayed by ELISA. Real-time quantitative PCR was performed on paired skin biopsies taken before and during RR, from 7 patients in the United States. Immunohistochmical staining was performed on paraffin sections of the same paired biopsies, using antibodies to CXCL10 and its receptor, CXCR3.
Results: Measurements of serum ELISA levels of CXCL10 in sequential, monthly specimens from 20 borderline (BL and BT) patients revealed significantly elevated levels of this chemokine associated with RR (p = 0.03). Real-time quantitative PCR revealed elevated expression of CXCL10 in skin biopsies during RR compared to pre-RR biopsies in 7/7 patients. Immunohistochemical staining of skin biopsies did not identify an increase in the number of leukocytes strongly positive for CXCL10 or its receptor, CXCR3, but suggested an overall increase in staining for both of these molecules throughout the infiltrate.
Conclusions: Together, these findings suggest that increased CXCL10 is a characteristic of cutaneous and systemic manifestations of RR. These findings may offer new possibilities for laboratory support in the diagnosis and monitoring of RR, and suggest that studies of the regulation of CXCL10 may provide further insight into the mechanisms responsible for this complication of leprosy.

1346 Flow Cytometric Applications for Virus Detection in the Clinical Microbiology Laboratory: Enterovirus as a Prototype

RC She, SN Preobrazhensky, CA Petti, DW Bahler. University of Utah School of Medicine, Salt Lake City, UT; ARUP Laboratories, Salt Lake City, UT.
Background: Culture and subsequent serotyping of human enteroviruses by fluorescence microscopy are both time-consuming and labor-intensive. The use of flow cytometry to detect virally infected cells has the potential of being more rapid, sensitive, and objective but has not been previously applied to enterovirus detection and serotyping.
Design: Primary monkey kidney (PMK) cells inoculated with several EV serotypes were trypsinized, fixed and permeabilized for staining with enterovirus-specific antibodies. Single color flow cytometry analysis was performed using an FC 500 instrument analyzing 5000 events. Kinetic studies of coxsackievirus B1 and echovirus 30 infection of PMK cells were performed on days 1-4 after inoculation and correlated with indirect fluorescence antibody (IFA) results.
Results: Echovirus 6, 11, and 30 infected cells were positive by flow cytometry for pan-enterovirus (Pan) and echovirus blend (EB) antibodies and negative for polio blend (PB), enterovirus blend (EVB), coxsackievirus B blend (CB), and isotype control (IC) antibodies. Coxsackievirus B1 infected cells were positive for Pan, CB, and coxsackievirus B1 antibodies and negative for PB, EVB, and IC antibodies. Results correlated with IFA in all cases but flow cytometry detected positive cells one day earlier than IFA. Figure 1. Rate of infection of PMK cells by coxsackievirus B1.

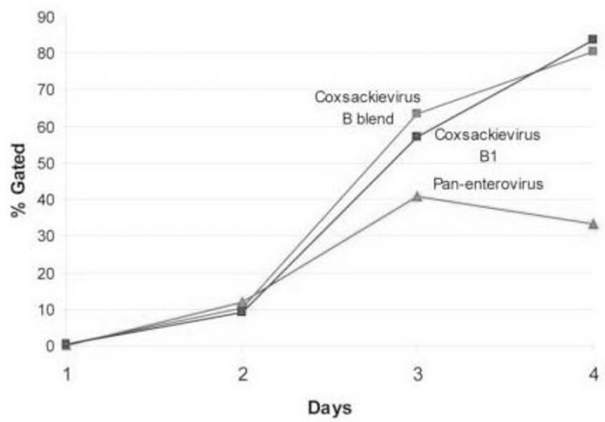

Conclusions: Flow cytometry can be effectively used for detecting enterovirus-infected cells in a laboratory setting. The potential advantages of flow cytometry over fluorescent microscopy include better quantitation of low levels of infection and earlier detection of virally infected cells in culture systems. These could lead to faster laboratory identification of pathogenic viruses. Additional studies are still needed to extend this method to other viruses and optimize detection strategies.

1347 Pathologic Studies of Leptospirosis, Ten-Years Experience at Centers for Disease Control and Prevention

W-J Shieh, P Chris, J Guarner, SR Zaki. Centers for Disease Control and Prevention, Atlanta, GA; Children's Hospital of Atlanta, Emory University, Atlanta, GA.

Background: Leptospirosis is a zoonotic disease caused by spirochetes of the genus *Leptospira*. It is a common infection affecting many species of wild and domestic animals worldwide. Human infection can occur either through direct contact with infected animals or more commonly through indirect contact with water or soil contaminated with the urine of infected animals. Pathologic studies are rarely performed and the pathogenesis of leptospirosis remained largely unknown.

Design: One hundred and sixty-five cases with positive immunohistochemical (IHC) test results for leptospira were identified from 1998–2008 database at Infectious Disease Pathology Branch, CDC. Although a few cases were from the US, most came from South America, Central America, and South East Asia. Histopathologic evaluation on available tissue samples was performed. The IHC assay was an indirect immunoalkaline phosphatase technique with a mixture of 16 rabbit polyclonal anti-leptospira antisera. Steiner's silver stain was also performed on selected cases.

Results: Histopathologic changes in the liver included hyperplasia of Kupffer cells, mild to moderate inflammatory infiltrate in portal tracts, and occasional hepatocellular necrosis. The lung frequently showed prominent intra-alveolar hemorrhage. The most consistent histopathology was a diffuse tubulointerstitial inflammation in the kidney, characterized by a mixed infiltrate of inflammatory cells. Although silver stains can highlight leptospires in tissues, they were not able to demonstrate fragments of bacteria disintegrated by host response or antibiotics treatment. IHC assay readily demonstrated granular, short filamentous, or spirochetal immunostaining of bacterial antigens, and is more useful for diagnosis.

Conclusions: The diagnosis of leptospirosis suspected by history and clinical manifestations can be supported by histopathologic findings, including interstitial nephritis and pulmonary hemorrhage. However, these features can occur in a variety of viral and bacterial infections. Silver stains are generally not a sensitive method for diagnosis because the detection of leptospires can be confounded by duration of illness and antibiotics treatment. IHC assay can detect leptospiral antigens in tissues and is a more sensitive and specific method for diagnosis. It is also instrumental for the studies of pathogenesis of leptospirosis.

1348 Activated Protein C Substantially Improves Survival in a Baboon Model of Anthrax-Mediated Sepsis

DJ Stearns-Kurosawa, V Collins, S Freeman, S Kurosawa. Boston University School of Medicine, Boston, MA.

Background: A fulminant septic response contributes to the lethality of toxigenic, Gram positive, *Bacillus anthracis*, the cause of clinical anthrax, but few studies address adjunctive therapeutics that might influence disease severity and mortality after infection. In ongoing studies, this model recapitulates the coagulopathic, inflammatory and metabolic pathophysiological changes in a manner similar to humans, with the lung as a primary target organ. The current study evaluates whether pre-treatment with recombinant activated protein C, a potent anti-coagulant and anti-inflammatory drug, influences outcome or disease severity in this model of anthrax bacteremia.

Design: Anesthetized nonhuman primates (*Papio c. cynocephalus*; n=40; 6-8kg) were pre-treated with recombinant activated protein C (DAA, drotrecogin alfa (activated)) followed by challenge with i.v. bacteria infusion. Some baboons were challenged with *B.anthracis* Sterne strain which produces anthrax toxins (n=32; toxemia + sepsis); some were challenged with *B.anthracis* Delta Sterne strain which does not produce toxins (n=8; sepsis only). The effect of DAA on baboon septic responses was determined by monitoring on-line physiologic responses, inflammation, coagulation, organ responses and survival.

Results: All baboons challenged with lethal doses of *B. anthracis* Delta Sterne strain survived as a result of DAA treatment ($p<0.01$). Challenge with Delta Sterne strain induced a typical septic response and DAA pre-treatment was accompanied by reduced coagulopathy, inflammation and pulmonary injury. The influence of DAA pre-treatment on animal responses after challenge with toxigenic Sterne strain was related to whether lethality was driven by sepsis or acute pulmonary injury. DAA ameliorated the later responses (>24hrs) due to sepsis and these animals survived ($p<0.05$), but treatment did not influence the early pulmonary failure (<24 hrs) which may be governed by exotoxin activities.

Conclusions: Death due to infection with *B. anthracis* is governed by both septic responses and the activities of anthrax exotoxins. Pre-treatment with DAA was highly effective in preventing death due to anthrax-mediated sepsis, but did not alter the very early deaths that may be attributable to exotoxins and/or other bacterial virulence factors. Thus, an effective therapeutic approach for treatment of *B.anthracis* infection will need to provide relief for the pathogenic effects of both anthrax toxins and host septic responses. [NIH RO1AI058107, U19AI062629 (SK)]

1349 Sepsis Induces Extensive Autophagy and Mitochondrial Damage in Human and Mouse Liver

PE Swanson, E Watanabe, JT Muenzer, RS Hotchkiss. University of Washington, Seattle, WA; Washington University, St. Louis, MO.

Background: Autophagy is a regulated process by which a cell degrades and recycles its own components; it can be triggered as an adaptive response during times of stress. Incorporation of organelles and cytoplasm into lysosomes (autolysosomes/autophagosomes) constitutes morphologic evidence of this process. The purpose of this study was to determine to what extent organellar damage and autophagy occurs in hepatocytes during sepsis.

Design: Electron microscopy (EM) was performed on post-mortem liver samples from 6 septic patients (obtained within 90 minutes of death) and from 4 control patients who had elective liver resection. Liver specimens were also obtained 24 hours after surgery from 4 sham-operated mice and 4 mice with sepsis surgery (cecal ligation and puncture - CLP). All samples were fixed and processed in a routine fashion. The number of autophagosomes was derived from 2500x magnification survey images (~3000 μ^2) to avoid sample bias; counts were performed in a blinded fashion on randomly sequenced images. Patterns of organellar injury were based on higher magnification images (15000-40000x) that were biased in favor of abnormal findings.

Results: Autophagosomes were more numerous in septic patients: 5.3 ± 3.3 vs. 1.2 ± 1.5 (mean ± SD) autophagosomes per image in sepsis vs. controls, respectively ($p<0.001$). Mitochondrial membrane abnormalities, including herniation of outer membranes into adjacent organelles, vacuolar change in cristae and myelin figures were seen in sepsis samples, but not controls. Nuclei and other hepatocyte organelles showed no consistent abnormality. Residual bodies were not more common in sepsis. Murine sepsis paralleled human studies, with 38.7 ± 3.9 and 7.2 ± 1.9 autophagosomes in septic and sham mice, respectively ($p = 0.002$). Autophagosomes incorporated lipid droplets in murine, but not human, samples. Neither necrotic nor apoptotic cell death was observed.

Conclusions: Hepatocyte autophagosomes are increased during sepsis in both humans and mice. The reproducible presence of mitochondrial membrane changes suggests both a source of organellar material in sepsis-induced autophagy and an underlying pattern of sepsis-related cell injury. The similarities between human and murine samples emphasizes the value of murine CLP-induced sepsis as a model of human disease.

Informatics

1350 Utility of VIPER (Virtual Imaging for Pathology, Education & Research) in Continuing Medical Education and Slide Surveys

T Barr, K Nicol, D Billiter, K Wohlever, P Baker, V Prasad. Nationwide Children's Hospital, Columbus, OH; Ohio Supercomputer Center, Columbus, OH.

Background: Current slide survey programs utilize glass slides for continuing medical education and are fraught with challenges. Examples include difficulty obtaining, cutting, staining, and shipping of multiple glass slides, inability to annotate slides and potential for discrepancy among slides due to loss of tissue in deeper sections. Digital pathology systems provide high-quality images that correspond to entire glass slides and provide image quality equivalent to a microscope. Use of digital pathology in teaching venues addresses these issues with slides by reducing the quantity of tissue and slides required, permitting multiple annotations and allowing all participating pathologists to review the same image.

Design: Virtual Imaging for Pathology, Education, & Research (VIPER) is a web-based application designed to facilitate digital reviews of whole slide images, providing an interface to whole slide images, pathology reports, and custom forms. Same images can be viewed independently or simultaneously. VIPER utilizes a relational database system capturing review data, generating multiple reports of interest. VIPER Team has partnered with a Supercomputer Center which contains an infrastructure providing high capacity data storage, a high performing network, and the ability to access high performance computing. We have had success with in-house pathologist review of web based images.

Results: There are challenges with established working groups adapting to new technology. Minimal training quickly improved the acceptance and comfort in utilizing digital images rather than the microscope and glass slides.

Conclusions: Benefits of providing high quality digital images in a custom application for educational prevails over traditional methods as it is cost effective. Digital technology enhances the learning experience by allowing multiple annotations as well as allowing multiple users to view the same image from different physical locations simultaneously. The use of VIPER is already creating a digital archive of clinically annotated data sets providing continued value to the pathology community. In the future these data sets could be utilized for continuing medical education, pathology reviews and research.

1351 Case of the Month and the Virtual Slidebox Implementation

V Brodsky, A Louissaint, J Gilbertson, Y Yagi. Massachusetts General Hospital, Boston, MA.

Background: Currently, a large volume of surgical pathology cases deemed interesting and often received from different countries are reviewed during the daily "Outs" conference with the residents and fellows of the Massachusetts General Hospital's Pathology department. These slides are subsequently filed for storage or returned to sender and are not necessarily easily retrievable for later review. We have built a searchable database driven collection of whole slide images of the slides presented at these conferences, accessible via a web interface. Additionally, selected surgical pathology cases with the associated added clinical history are submitted into a queue by the residents, with one case picked and published monthly on the "Case of the Month" website.

Design: The development platform corresponding with the Massachusetts General Hospital website includes Microsoft Windows Server 2008 and Microsoft SQL Server Developer Edition. The Case of the Month website is built on the open source ASP-based Blogengine 1.4 with modifications allowing for submission queuing prior to final approval. The slides are scanned with 0.33um/pixel sampling period using Mirax Scan device (3DHISTECH Ltd, Carl Zeiss Microimaging GmbH) and are put on a dedicated storage server, each linked from the 3DHISTECH's Mirax Server database software, which provides its own Virtual Slidebox web interface as well as allowing for links from the Case of the Month website to target individual slides. Clicking on the link to the whole slide image in the browser opens the Mirax Viewer which lets the user navigate the whole slide image streaming from the server.

Results: The interactions with the scanner and the website are currently agreed to be valuable additions to the resident education. The 0.33um/pixel sampling period of the scanned slides appears sufficient for surgical cases and is considerably higher than the resolution of printed histological atlases, however the possibility of scanning cytology